Variations in Semiconducting Polymer Microstructure and Hole Mobility with Spin-Coating Speed

Dean M. DeLongchamp,* Brandon M. Vogel, Youngsuk Jung, Marc C. Gurau, Curt A. Richter, Oleg A. Kirillov, Jan Obrzut, Daniel A. Fischer, Sharadha Sambasivan, Lee J. Richter, and Eric K. Lin

National Institute of Standards and Technology, Gaithersburg, Maryland 20899-8541

Received June 23, 2005
Revised Manuscript Received September 16, 2005

Interest in organic semiconductors has increased because of their potential use in new electronics applications such as radio frequency identification tags, biosensors, or photovoltaics. The development of solution processable organic semiconductors has made it possible to take advantage of low-cost processing methods such as spin coating, dip coating, or ink-jet printing onto flexible substrates.[1] However, the performance of these materials in devices is difficult to control and new processing methods can deliver unexpected results. These deviations are often due to variability in film microstructure that leads to variability in carrier transport properties. The microstructure is sensitive to processing variables because they influence the dynamic assembly process of the material as it dries from a solution to a solid thin film that is crystalline or semicrystalline.

Regioregular poly(3-hexylthiophene) (P3HT), a solution processable semiconducting polymer, exemplifies these large variations with processing conditions. The microstructure of P3HT films is sensitive to the regioregularity of the polymer,[2] its molecular weight (MW),[3−6] and its casting solvent.[7,8] In field effect transistors (FETs), the highest hole mobilities are achieved in P3HT films with chains that are preferentially π-stacked in crystalline lamellae with the (010) lattice direction oriented in the source-drain (substrate) plane,[2,7] allowing for efficient hole delocalization and transport. In general, this microstructure is attained with a highly regioregular P3HT[2,7] cast from low-volatility solvents.[8] The edge-on planar orientation is thought to be thermodynamically preferred for regioregular P3HTs,[2,7,8] but there is no comprehensive understanding of how this structure develops.

Variations in the spin-coating process may be a source of differences in the P3HT microstructure because they may shift complex balance of inertial forces and solvent evaporation during the solidification of the film from solution.[9] The morphology of semicrystalline polymers such as regioregular P3HT is affected by the rate of solidification; slower solvent removal rates result in materials closer to their equilibrium structure. Because the solvent evaporation rate during spin coating is proportional to the spin speed,[9] changes in spin speed provide a method to systematically vary the solvent evaporation rate. In this communication, we report the influence of the rotational speed of the spin-coating process on the orientation of the P3HT conjugated plane from films cast from chloroform solutions.

Regioregular P3HT films (18 kDa, Plextronics,[28] by GRIM, >99% regioregular)[10] were prepared by spin coating at (250 to 4000) 2π rad/min [hereafter, we use the common unit "revolutions per minute" (rpm) to refer to 2π rad/min] with 10 000 rpm/s acceleration from solutions of 2, 4, and 6 mg/mL in anhydrous chloroform. Films were prepared on silicon oxide surfaces, and surfaces that were modified with hexamethyldisilazane (HMDS). To quantify structural changes, we employ synchrotron-based near-edge X-ray absorption fine structure (NEXAFS) spectroscopy,[11] which measures the soft X-ray excitation of 1s electrons to unfilled molecular orbitals. The carbon 1s $\rightarrow \pi^*$ excitation of conjugated systems exhibits a strong NEXAFS absorbance,[12,13] and soft X-ray polarization allows the determination of the average π^* orbital orientation[14,15] and the P3HT conjugated plane orientation. NEXAFS spectra were collected in partial electron yield (PEY) mode to probe the topmost $\approx$10 nm of the films.

We find that the P3HT conjugated plane varies from an edge-on to a plane-on orientation depending on the spin speed employed. NEXAFS spectra representing both orientation limits are shown in Figure 1a. The primary carbon K-edge resonances are the carbon−carbon 1s $\rightarrow \pi^*$ at 285.3 eV, the superimposed carbon−hydrogen and carbon−sulfur 1s $\rightarrow \sigma^*$ at 287.8 eV, and the carbon−carbon 1s $\rightarrow \sigma^*$ at 293 and 303 eV. The carbon−carbon 1s $\rightarrow \pi^*$ resonance exhibits a strong systematic variation with incident angle that indicates conjugated plane orientation. In the film spun at 250 rpm, the 1s $\rightarrow \pi^*$ absorbance intensity is greatest at 70° incidence, indicating that π^* orbitals are preferentially oriented

* To whom correspondence should be addressed. E-mail: deand@nist.gov.

(1) Gamota, D. R.; Brazis, P.; Kalyanasundaram, K.; Zhang, J. *Printed Organic and Molecular Electronics*; Kluwer Academic Publishers: New York, 2004.
(2) Sirringhaus, H.; Brown, P. J.; Friend, R. H.; Nielsen, M. M.; Bechgaard, K.; Langeveld-Voss, B. M. W.; Spiering, A. J. H.; Janssen, R. A. J.; Meijer, E. W.; Herwig, P.; de Leeuw, D. M. *Nature* **1999**, *401*, 685.
(3) Kline, R. J.; McGehee, M. D.; Kadnikova, E. N.; Liu, J. S.; Fréchet, J. M. J. *Adv. Mater.* **2003**, *15*, 1519.
(4) Zen, A.; Pflaum, J.; Hirschmann, S.; Zhuang, W.; Jaiser, F.; Asawapirom, U.; Rabe, J. P.; Scherf, U.; Neher, D. *Adv. Funct. Mater.* **2004**, *14*, 757.
(5) Goh, C.; Kline, R. J.; McGehee, M. D.; Kadnikova, E. N.; Frechet, J. M. J. *Appl. Phys. Lett.* **2005**, 86.
(6) Kline, R. J.; McGehee, M. D.; Kadnikova, E. N.; Liu, J. S.; Frechet, J. M. J.; Toney, M. F. *Macromolecules* **2005**, *38*, 3312.
(7) Bao, Z.; Dodabalapur, A.; Lovinger, A. J. *Appl. Phys. Lett.* **1996**, *69*, 4108.
(8) Chang, J. F.; Sun, B. Q.; Breiby, D. W.; Nielsen, M. M.; Solling, T. I.; Giles, M.; McCulloch, I.; Sirringhaus, H. *Chem. Mater.* **2004**, *16*, 4772.
(9) Meyerhofer, D. *J. Appl. Phys.* **1978**, 3993.
(10) Loewe, R. S.; Khersonsky, S. M.; McCullough, R. D. *Adv. Mater.* **1999**, *11*, 250.
(11) Stöhr, J. *NEXAFS Spectroscopy*; Springer-Verlag: Berlin, 1992.
(12) Yokoyama, T.; Seki, K.; Morisada, I.; Edamatsu, K.; Ohta, T. *Phys. Scr.* **1990**, *41*, 189.
(13) Agren, H.; Vahtras, O.; Carravetta, V. *Chem. Phys.* **1995**, *196*, 47.
(14) Frey, S.; Stadler, V.; Heister, K.; Eck, W.; Zharnikov, M.; Grunze, M.; Zeysing, B.; Terfort, A. *Langmuir* **2001**, *17*, 2408.
(15) Wu, W. L.; Sambasivan, S.; Wang, C. Y.; Wallace, W. E.; Genzer, J.; Fischer, D. A. *Eur. Phys. J. E* **2003**, *12*, 127.

10.1021/cm0513637 CCC: $30.25
Published on Web 10/13/2005

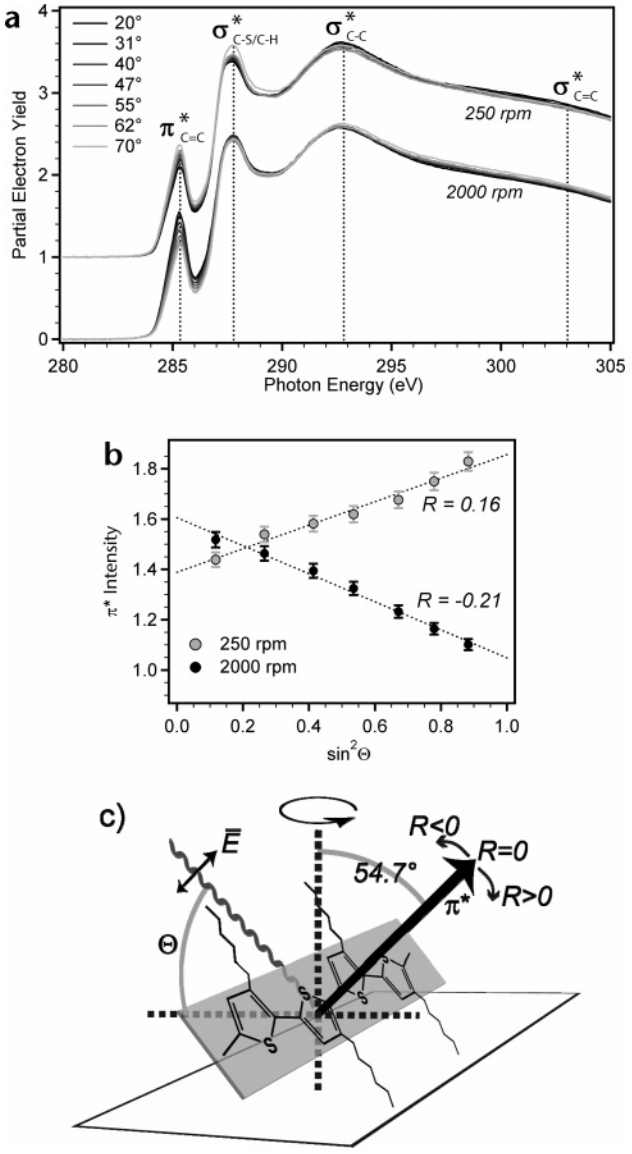

Figure 1. (a) Carbon K-edge NEXAFS spectra for P3HT films spun at 250 and 2000 rpm from a 2 mg/mL chloroform solution, with varying incident angle Θ. Standard experimental error for PEY and its integrated intensity is <2%. (b) Analysis of π^* intensity data, showing extrapolation to 0° and 90°. Uncertainty for R is the standard deviation of a direct fit. (c) The π^* transition is perpendicular to the conjugated plane. Data are for films atop unmodified SiO_2.

parallel to the substrate and that the conjugated plane is preferentially oriented edge-on. In the film spun at 2000 rpm, the conjugated plane is preferentially oriented plane-on.

The P3HT side chain orientation is consistent with the conjugated plane orientation, but it is weaker. In the film spun at 250 rpm, the 293 eV resonance is greatest at 20° incidence, indicating that the carbon−carbon σ^* orbitals are preferentially oriented out of the substrate plane. Because these orbitals are primarily along the side chains, the side chains must be out of the substrate plane, consistent with the edge-on conjugated plane. The angular variation of the carbon−hydrogen 1s → σ^* resonance (perpendicular to the side chains) does support this orientation, although this resonance is convoluted with the carbon−sulfur 1s → σ^* resonance. These trends are reversed in the film spun at 2000 rpm, indicating that the side chains preferentially lie in the substrate plane, consistent with the plane-on conjugated plane.

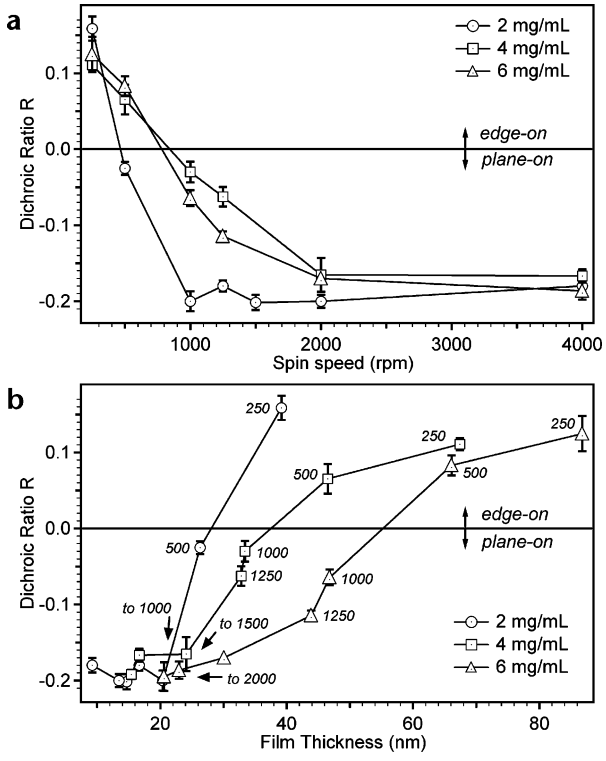

Figure 2. Dichroic ratio R as a function of (a) spin speed and (b) thickness. For part b, spin speed is indicated near the data points. Positive R values indicate edge-on orientation of the conjugated plane, while negative R values indicate plane-on orientation. Data are for films atop unmodified SiO_2. Error bars are standard deviations based on fit statistics.

To quantify the conjugated plane orientation, we define a dichroic ratio, $R = (I_{90°} - I_{0°})/(I_{90°} + I_{0°})$, where $I_{90°}$ and $I_{0°}$ are the intensities at 90° and 0° incidence, linearly extrapolated from the data with incident angle, as shown in Figure 1b.[11] The R values can vary from ≈0.7 ($R = 1$ is not possible because of a finite X-ray polarization) to −1, with more positive values indicating a greater edge-on conjugated plane orientation, as illustrated in Figure 1c. As the samples are not likely represented by a single, uniform orientation, the observed R values reflect an average of the edge-on, plane-on, and amorphous orientations present. $R = 0$ represents a net balance (azimuthally averaged) of different orientations, while positive or negative R values represent a preferential bias of the orientation distribution.

In Figure 2a, R is shown as a function of spin speed. In general, films cast using slow spin speeds exhibit more edge-on orientation, films cast using fast spin speeds exhibit more plane-on orientation, and the orientation varies smoothly between these limits. In Figure 2b, R is shown as a function of film thickness, which is dependent on both solution concentration and spin speed, to account for any orientation differences due to film thickness. For a given film thickness, lower concentration solutions exhibit more edge-on orientation than higher concentration solutions. Similar trends were observed for films cast atop HMDS-coated substrates. Spectral ellipsometry measurements (from the $\pi-\pi^*$ transition) of poly(3-octylthiophene) films have shown that the long axis anisotropy decreases slightly as film thickness increases.[16,17] The NEXAFS data suggest that the conjugated plane orientation is independent of this long axis anisotropy.

Although P3HT molecular orientation changes with spin speed, there is not a strong variation in the film surface morphology. Atomic force microscopy (AFM) images were collected from films over the full range of observed R values (see Supporting Information). Regardless of the spin speed, we observe textured surfaces similar to those of chloroform-cast, moderate MW P3HT films described as "nodular"[3,6] or "granular".[8] Surface morphology does not correlate to R, aside from a slight decrease in nodule size at more negative R. We do not observe needlelike crystals[3,6,18] nor nanoribbons.[8] The variation of the conjugated plane orientation with spin speed is not due to the crystallinity or surface roughness observed for low-MW P3HT[3,6] or films cast from low-volatility solvents.[8,18]

The FET saturation field effect mobility is correlated to the P3HT conjugated plane orientation determined by NEXAFS. FET performance was evaluated from transfer characteristics collected for P3HT films spun at three conditions: (1) 2 mg/mL at 250 rpm ($R = 0.16$), (2) 4 mg/mL at 1250 rpm ($R = -0.07$), and (3) 6 mg/mL at 2000 rpm ($R = -0.20$). These conditions result in films ≈30 nm thick, each with a different microstructure. Gold bottom contact FET test beds with HMDS-treated gate oxides were used with variations in channel length from 10 to 100 μm and channel width from 0.2 to 1.0 mm. Saturation regime analysis was performed[19] on ≈100 FET devices per spin condition. The mean saturation field effect mobility was 1×10^{-3} cm^2/(V·s) for condition 3, the fastest spin speed. Mobility improved to 2×10^{-3} cm^2/(V·s) for condition 2, the intermediate spin speed. Finally, mobility was highest at 6×10^{-3} cm^2/(V·s) for condition 1, the slowest spin speed. The statistical variation of mobility is not Gaussian, and the uncertainty is best described by the shapes of the distributions (see Supporting Information). The higher hole mobility is attributed to the greater edge-on orientation, which presumably indicates better $\pi-\pi$ overlap in the source-drain plane. The surface-sensitive NEXAFS measurements are consistent with the expected molecular organization at the buried dielectric interface based upon the device characteristics. The 6-fold increase in mobility between fast and slow spin conditions is comparable to reported mobility improvements from spin-cast to drop-cast films.[2,7,20]

The correlation of the orientation with spin speed, but not film thickness, suggests that the systematic variation of the conjugated plane orientation is related to changes in the solvent evaporation rate. The slowest spin speeds in this study resulted in more edge-on orientation. Similarly, slowly solution casting or dip casting P3HT films typically results in a high degree of edge-on orientation.[7,20−22] In addition, P3HT films spin cast or solution cast from low-volatility solvents are more crystalline, with more efficient interchain π stacking and more edge-on orientation, than films prepared from high-volatility solvents.[8,23] The adoption of a preferred plane-on orientation at fast spin speeds is more difficult to understand because rapid drying often results in a disordered material ($R = 0$). It is possible that disklike or rodlike aggregates form in solution[24−26] and may assemble on the surface with a plane-on molecular orientation before any significant crystallization or molecular reorganization occurs. Alternatively, plane-on orientation may arise from amorphous regions of the film, which are anisotropic.[23] The differences in film microstructure observed here may be the source of some of the variation in P3HT performance among published studies. Other processing variables that affect the rate of solvent evaporation during spin coating such as the air flow conditions and the solvent saturation of the spin environment[27] are also likely to change microstructure and field effect mobility. Because most additive patterning processes envisioned for solution-processable semiconductors will include a drying step, control over the drying rate should be carefully considered in any process design.

Acknowledgment. D.M.D., B.M.V., and M.C.G. acknowledge support from the NRC-NIST postdoctoral fellowship program.

Supporting Information Available: Thickness vs spin speed, experimental details, AFM micrographs, and electrical measurements. This material is available free of charge via the Internet at http://pubs.acs.org.

CM0513637

(16) Zhokhavets, U.; Gobsch, G.; Hoppe, H.; Sariciftci, N. S. *Synth. Met.* **2004**, *143*, 113.
(17) Zhokhavets, U.; Gobsch, G.; Hoppe, H.; Sariciftci, N. S. *Thin Solid Films* **2004**, *451−452*, 69.
(18) Yang, H. C.; Shin, T. J.; Yang, L.; Cho, K.; Ryu, C. Y.; Bao, Z. N. *Adv. Funct. Mater.* **2005**, *15*, 671.
(19) Gundlach, D. J.; Shur, M. S.; Jackson, T.; Kanicki, J.; Martin, S.; Dodabalapur, A.; Crone, B. Electrical Behavior of Organic Transistors and Circuits. In *Printed organic and molecular electronics*; Gamota, D., Brazis, P. W., Kalyanasundaram, K., Zhang, J., Eds.; Kluwer Academic Publishers: New York, 2004.
(20) Wang, G. M.; Swensen, J.; Moses, D.; Heeger, A. J. *J. Appl. Phys.* **2003**, *93*, 6137.
(21) Aasmundtveit, K. E.; Samuelsen, E. J.; Guldstein, M.; Steinsland, C.; Flornes, O.; Fagermo, C.; Seeberg, T. M.; Pettersson, L. A. A.; Inganas, O.; Feidenhans'l, R.; Ferrer, S. *Macromolecules* **2000**, *33*, 3120.
(22) Hugger, S.; Thomann, R.; Heinzel, T.; Thurn-Albrecht, T. *Colloid Polym. Sci.* **2004**, *282*, 932.
(23) Breiby, D. W.; Samuelsen, E. J. *J. Polym. Sci., Part B: Polym. Phys.* **2003**, *41*, 2375.
(24) Yue, S.; Berry, G. C.; McCullough, R. D. *Macromolecules* **1996**, *29*, 933.
(25) Yamamoto, T.; Komarudin, D.; Arai, M.; Lee, B. L.; Suganuma, H.; Asakawa, N.; Inoue, Y.; Kubota, K.; Sasaki, S.; Fukuda, T.; Matsuda, H. *J. Am. Chem. Soc.* **1998**, *120*, 2047.
(26) Kiriy, N.; Jahne, E.; Adler, H. J.; Schneider, M.; Kiriy, A.; Gorodyska, G.; Minko, S.; Jehnichen, D.; Simon, P.; Fokin, A. A.; Stamm, M. *Nano Lett.* **2003**, *3*, 707.
(27) Kim, D. H.; Park, Y. D.; Jang, Y.; Kim, S.; Cho, K. *Macromol. Rapid Commun.* **2005**, *26*, 834.
(28) Certain equipment, instruments, or materials are identified in this paper to adequately specify the experimental details. Such identification does not imply recommendation by the National Institute of Standards and Technology nor does it imply the materials are necessarily the best available for the purpose.